UDC 629.5 https://doi.org/10.15407/itm2023.04.003

V. K. SHAMAKHANOV, S. V. KHOROSHYLOV

MODELING CABLE-PULLEY DEPLOYMENT SYSTEMS OF TRANSFORMABLE ROD STRUCTURES

Institute of Technical Mechanics
of the National Academy of Sciences of Ukraine and the State Space Agency of Ukraine,
15 Leshko-Popel St., Dnipro, 49005, Ukraine; e- mail: 1luckyminerfriends1@gmail.com

Метою статті є розробка спрощеного метода моделювання тросових систем розгортання стрижневих систем, що дозволяє визначити натяг тросів та вузлові рушійні сили з урахуванням тертя та інших особливостей розглянутої системи.

При проведенні досліджень використані методи теоретичної механіки, систем зв'язаних тіл, чисельного розв'язання систем диференційних рівнянь та комп'ютерного моделювання.

Розглянута задача розробки спрощеного методу моделювання тросових систем розгортання стрижневих конструкцій. Запропоновано визначати вузлові рушійні сили шляхом розрахунку натягу тросів з урахуванням тертя та інших особливостей стрижневої конструкції, тросів та шківів.

При створенні моделі тросової системи розгортання в якості об'єкта дослідження було обрано стрижневу систему, яка представляє собою дві секції опорної ферми рефлектора, що трансформуються. Кожна секція формується із діагональних та горизонтальних стрижнів трубчатого поперечного перерізу. Секції поєднані між собою шарнірними вузлами. Конструкція розгортається за допомогою верхнього та нижнього тросів, що проходять через систему шківів та натягуються за допомогою електродвигуна. Зусилля, що розгортають, реалізуються шляхом передачі конструкції сил натягу троса за рахунок статичного тертя та тиску між тросом та шківами. Для подальшої реалізації моделі у програмному пакеті з відкритим кодом зроблено деякі спрощення, які обумовлені складністю конструкції.

Розроблено спрощений метод розрахунку вузлових рушійних сил при моделюванні розгортання стрижневих конструкцій за допомогою тросів. Отримано залежності натягу, подовження, послаблення та зміни нейтральної довжини троса від часу, а також зміни з часом сил, що передаються шківам від троса. З використанням цих результатів проведено комп'ютерне моделювання процесу розгортання стрижневої конструкції для випадку постійної швидкості намотки тросів лебідкою. Результати дають змогу контролювати час та швидкість розгортання стрижневих систем в залежності від характеристик та сил натягу тросів.

Запропонований підхід реалізовано з використанням загально доступного програмного забезпечення. Цей підхід дозволяє забезпечити гнучкість моделювання та скоротити час створення та розрахунку моделей.

Ключові слова: *тросова система розгортання; конструкції, що трасформуються; багатотільна динаміка; відкрите програмне забезпечення; гнучкий стрижень.*

The aim of this article is to develop a simplified method for modeling cable-pulley deployment systems of rod structures based on the calculation of cable tensions and nodal driving forces with account for friction and other features of the system.

Methods of theoretical mechanics, multibody dynamics, numerical integration of differential equations, and computer modeling were used during the research.

The task of developing a simplified approach to modeling cable-pulley deployment systems for rod structures is considered. It is proposed to determine nodal driving forces by calculating cable tensions with account for friction and other features of the cable-pulley system, cables, and pulleys.

To develop a model of cable-pulley deployment system, a rod system was chosen as the research object, which represents two sections of the transformable support truss of a reflector. Each section consists of diagonal and horizontal rods with tubular cross-sections. The sections are interconnected by hinge units. The structure is deployed using an upper and a lower cable, which pass through pulleys and are tensioned by an electric motor. The deploying forces are implemented by transferring the cable tension forces to the structure due to static friction and pressure between the cables and the pulleys. For further implementation of the model in an open-source software package, some simplifications were made due to the complexity of the design.

A simplified method was developed for nodal driving force calculation in simulating rod structure deployment with the help of cables. The tensions, elongations, slacks, and neutral length of the cables and the forces transmitted from the cables to the pulleys were calculated as a function of time.

Using them, the deployment of a rod structure was simulated for a constant cable speed. The results make it possible to control the rod system deployment time and rate depending on the characteristics and tension forces of the cables.

The proposed approach is implemented using open-source software, and it provides modeling flexibility and reduces the model development and run time.

Keywords: *cable-pulley deployment system, transformable structures, multibody dynamics, open-source software, flexible rod.*

Introduction. Structures with significant spatial dimensions, such as antennas [1] and booms [2], have been used for space applications. Due to the fact that the space under the fairing of the launch vehicle is limited, such structures are launched into orbit in a stowed state. Before operation they are deployed in such a way as to form the desired in-orbit configuration. But, unfortunately, there are known cases of abnormal deployment of such structures, which are primarily related to the complexity of the structures themselves and the difficulties of conducting full-scale experiments under the conditions of Earth's gravity. The listed features encourage engineers and researchers to increasingly use mathematical and computer modeling methods to analyze similar structures.

Space structures can be implemented in the form of rod systems connected by hinges, which are deployed using cable-pulley systems.

The model of the Astromesh antenna was developed in Ref [3] using the its representation as a system of flexible bodies, where special attention was paid to the formulation of the cable-pulley system with friction based on Lagrange-Euler elements (ALE). This modeling method significantly reduced the number of generalized coordinates and made full-scale simulation of antenna dynamics possible.

In the article [4], the model of the flexible dynamics of the reflector is developed using the absolute nodal coordinate formulation (ANCF), which leads to a constant mass matrix without centrifugal and Coriolis forces. Then, this model is applied to simulate the phenomena of non-synchronous deployment of the reflector, taking into account the flexibility of the structure and the degradation of driving forces from the cable-pulley system. Simulation results show that non-synchronous deployment can increase the load on the struts of the reflector support ring.

The authors of the article [5] showed that the antenna deployment process is asynchronous because of the effect of degradation of the driving forces of the deployment cable system caused by pulley frictions. In addition, a significant growth of strain in the final stage greatly affects the smoothness of deployment. The phenomenon of non-synchronous deployment due to the structure flexibility and damping of the forces of the cable system was studied in Ref. [6]. The results show that this phenomenon can increase the stresses in the ring truss, which should be taken into account when designing the truss.

In work [7], the movement of active sliding cables is considered as kinematic constraints of the system from the point of view of multibody dynamics, and the general model of the structure deployment is created using differential algebraic equations (DAE). The proposed method is used to build a new control strategy for solving more general problems of deploying structures with fewer actuators.

Full-scale deployment simulation of space structures using cable-pulley systems is known to be challenging, as traditional contact-based methods require a fine mesh for the cables, a large number of contact detections, and integration with small steps [8, 9].

The authors of the article [10] proposed a new method of modeling systems made of cables and pulleys, which is based on dividing the cable into two seg-

ments: non-contact and contact ones, depending on which part of the rope is in contact with the pulley. The contactless segment consists of variable length elements based on ALE. The contact segment is considered an invisible segment intended to limit the variable length cable element on the pulley; its limit is dynamically determined by the relative configuration between the pulley and the cable.

On the basis of the dynamic analysis of the deployment of the AstroMesh antenna, a method for optimizing the strategy of winding the cable is proposed in Ref. [11]. Considering the effect of the cable properties and friction, the driving force for deployment is derived according to energy conservation. An optimization model was built with the aim to minimize driving power during the deployment, using the calculation variables consisting of the control parameters of the cable winding length curve.

Taking into account the above-mentioned difficulties, it is urgent to develop a simplified method for modeling cable-pulley deployment systems for rod structures, which allows obtaining analytical expressions for determining the driving forces and increasing the efficiency of calculations.

The aim of the article is to develop a simplified method for modeling cable-pulley deployment systems for rod structures, which is based on calculation of the cable tensions and nodal driving forces, taking into account friction and other features of the system.

Problem statement. Two sections of the transformable reflector support truss were chosen as the object for the study. Each section is formed from diagonal and horizontal rods with tubular cross-section. Sections are interconnected by hinged units (Fig. 1).

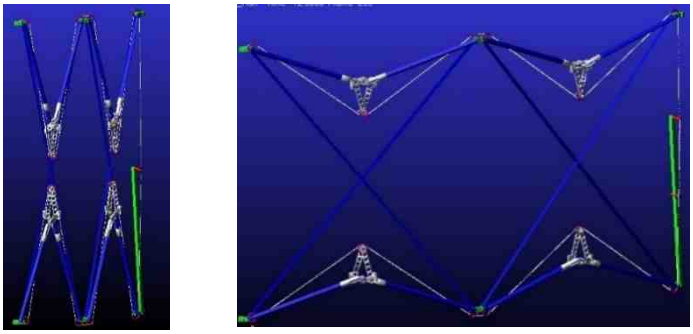

a) b)

Fig. 1 – Transformable structure (a – stowed state, b – deployed state)

The diagonal rods are connected in such a way that the rotation hinge provides rotation of one diagonal relative to the other. The upper and lower horizontal rods are connected to each other with the help of V-folding jounts, which ensure the transformation of the horizontal rods. Diagonal and horizontal rods are connected to each other with the help of hinge units.

The structure is deployed using an upper and lower cable passing through a system of pulleys and tensioned by an electric motor. The driving forces are applied to the structure by transferring the cable tension due to static friction and pressure between the cable and the pulleys. To simulate the deployment of the structure, it is necessary to determine the driving forces with which the cable acts on the corresponding pulleys in the hinge nodes, which lead to the movement of

the horizontal rods of the V-folding assembly. The approach for solving this problem are presented below.

Model of rod structure. The ANCF is used to model the rod structure. The ANCF method uses slope vectors to parameterize the orientation of the rod cross section instead of the rotation parameters. The orientation of the cross-section of the rod is described using conventional linear interpolation, and displacements along its axis are interpolated using linear shape functions. The slope vectors are derivative vectors with respect to the reference frame of the scaled linear base element. The definition of elastic forces is based on the Saint–Venant–Kirchhoff solid medium formulation, using the relationship between the nonlinear Green-Lagrange strain tensor and the second Piol–Kirchhoff stress tensor.

The geometry of the elastic rod element is defined by two nodes with slope vectors at each node and position. The degrees of freedom of the *i*-th node of the element are nodal displacements and variations of slope vectors. Each node has nine degrees of freedom, so a two-node linear rod element has the following 18 degrees of freedom

$$q^{(i)} = \left[u^{(i)T} \quad u_{\eta\eta}^{(i)T} \quad u_{\zeta\zeta}^{(i)T} \right]^T , \tag{1}$$

where $u^{(i)}$ is the nodal displacement, and $u_{\eta\eta}^{(i)}$, $u_{\zeta}^{(i)}$ are the slope vectors.

A flexible rod element is described by means of position vectors $r^{(i)}$, $r_{\zeta}^{(i)}$ and two slope vectors $r_{\eta}^{(i)}$ for each i-th node.

The hinge units that connect the sections together are modeled as several revolute joints connected to each other by ordinary rigid elements. For modeling, the main properties of these hinge assemblies are the stiffness, location and direction of the axes of rotation of the hinges.

The center of gravity of a rigid element is determined by the position vector in global coordinates, and serves as the reference point for specifying local coordinate values. A universal, adjustable hinge is used to model the V-folding joints that connects the horizontal rods. This hinge connects two bodies together and makes it possible to constrain 6 relative degrees of freedom, namely, movement along three axes of the local coordinate system of the connecting bodies and rotation around these axes. The constrain equations for this type of joints have the following form:

$$A^T (x_1 - x_2) = 0 , \tag{2}$$

where x_1, x_2 are the positions of the connection points in global reference frame on bodies 1 and 2, respectively; $A = (e_x^i \quad e_y^i \quad e_z^i)$ is the rotation matrix from the local coordinate frame of the hinge to the global coordinate frame.

Each equation in system (2) corresponds to a constrained direction, so if all directions are constrained, it simplifies as follows:

$$x_1 - x_2 = 0 , \tag{3}$$

because $A^T (x_1 - x_2) = 0 \leftrightarrow x_1 - x_2 = 0$.

If all rotational degrees of freedom are constrained, the equation of rotation has the following form:

$$\begin{pmatrix} e_y^j \cdot e_z^i \\ e_x^j \cdot e_z^i \\ e_x^j \cdot e_y^i \end{pmatrix} = \begin{pmatrix} 0 \\ 0 \\ 0 \end{pmatrix}. \tag{4}$$

For cases when the rotation is not limited around one of the axes, equation (4) takes the following form:

$$\begin{pmatrix} e_x^j \cdot e_z^i \\ e_x^j \cdot e_y^i \end{pmatrix} = \begin{pmatrix} 0 \\ 0 \end{pmatrix}, \begin{pmatrix} e_y^j \cdot e_z^i \\ e_y^j \cdot e_x^i \end{pmatrix} = \begin{pmatrix} 0 \\ 0 \end{pmatrix}, \begin{pmatrix} e_z^j \cdot e_y^i \\ e_z^j \cdot e_x^i \end{pmatrix} = \begin{pmatrix} 0 \\ 0 \end{pmatrix}, \tag{5}$$

for x, y, z axis, respectively.

The diagonal rods are connected to each other with the help of revolute joints, which limit all relative degrees of freedom between the two bodies, except the rotation around a local axis. The revolute joint is equivalent to a universal hinge in which all degrees of freedom are limited except for rotation around the local x-axis. Also, the revolute joint is used to connect horizontal and diagonal rods to the hinge assemblies. Rigid bodies are connected to each other by means of fixed joints, which constrain all degrees of freedom of the element in a defined local position. The fixed joint is equivalent to a universal hinge with all degrees of freedom constrained.

The folding sections are attached to a vertical rod, which is modeled by the same elastic beam element as the section rods, but with a larger diameter and cross-section. The vertical rod is connected to the hinge units of the first section by means of a rigid joint at the upper node and a sliding joint in the lower node. The sliding join ensures the movement of a point of one body along the longitudinal axis of the second body. The vector of degrees of freedom of the sliding joint (6) contains the sliding parameter, its time derivative, and the vector of Lagrange parameters. The first three Lagrange parameters represent the sliding forces in the global coordinate system, and the last three parameters are the sliding torques about the axes of the global coordinate system.

$$q = \begin{bmatrix} s & \dot{s} & \lambda_1 & \lambda_2 & \lambda_3 & \lambda_4 & \lambda_5 & \lambda_6 \end{bmatrix}. \tag{6}$$

Position vectors have the following form (7):

$$x^i = \begin{bmatrix} x_1^i & x_2^i & x_3^i \end{bmatrix}^T ; \; x^j = \begin{bmatrix} x_1^j & x_2^j & x_3^j \end{bmatrix}^T . \tag{7}$$

During initialization, the unit vectors of the global reference frame are transferred to the local frames of each body, thus vectors v_1^i, v_2^i, v_3^i for the first body and v_1^j, v_2^j, v_3^j for the second body are obtained. Equations of displacement and acceleration constraints, respectively (8), have the form:

$$\begin{bmatrix} r^i(x^i)-r^j(x^j) \\ \dfrac{\partial r^j(x^j)}{\partial x_1^j}\lambda \\ v_2^j v_3^i \\ v_3^j v_1^i \\ v_2^j v_1^i \end{bmatrix} = 0 \begin{bmatrix} \dfrac{\partial r^i(x^i)}{\partial t}-\dfrac{\partial r^j(x^j)}{\partial t}-\dfrac{\partial r^j(x^j)}{\partial x_1^j}\dot{s} \\ \dfrac{\partial r^j(x^j)}{\partial x_1^j}\lambda \\ \dot{v}_2^j v_3^i + v_2^j \dot{v}_3^i \\ \dot{v}_3^j v_1^i + v_3^j \dot{v}_1^i \\ \dot{v}_2^j v_1^i + v_2^j \dot{v}_1^i \end{bmatrix} = 0, \quad (8)$$

where r^i, r^j are the position vectors of the i-th and j-th bodies.

The dynamic model of the structure is obtained based on ANCF, taking into account the kinetic and elastic energies of the rods. The method of Lagrange multipliers is used to take into account the constraints. Finally, the model of the entire system is presented as a system of differential and algebraic equations as follows:

$$M\ddot{X} + C(X,t) + \Phi_X^T \Lambda = V(t),$$

$$\Phi(X) = 0,$$

where X is the state vector; M is the mass matrix; $C(X,t)$ is the vector representing the stiffness of the system; $V(t)$ is the vector of non-conservative generalized forces due to the action of the deployment system; Λ is the vector of Lagrange multipliers .

Model of the cable-pulley system. The deployment cable system is modeled to determine the driving forces with which the cable acts on the corresponding structural elements. The static friction and pressure between the cables and the pulleys are used to transmit the cable tension to the nodal forces deploying the structure, as shown in Fig. 2.

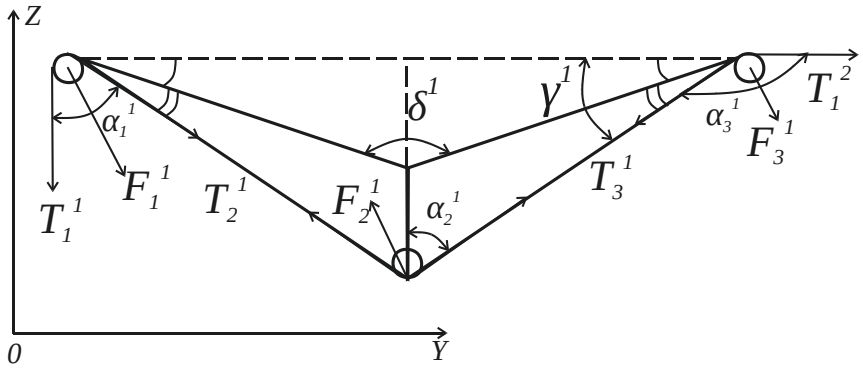

Fig. 2 – The directions of forces acting during deployment

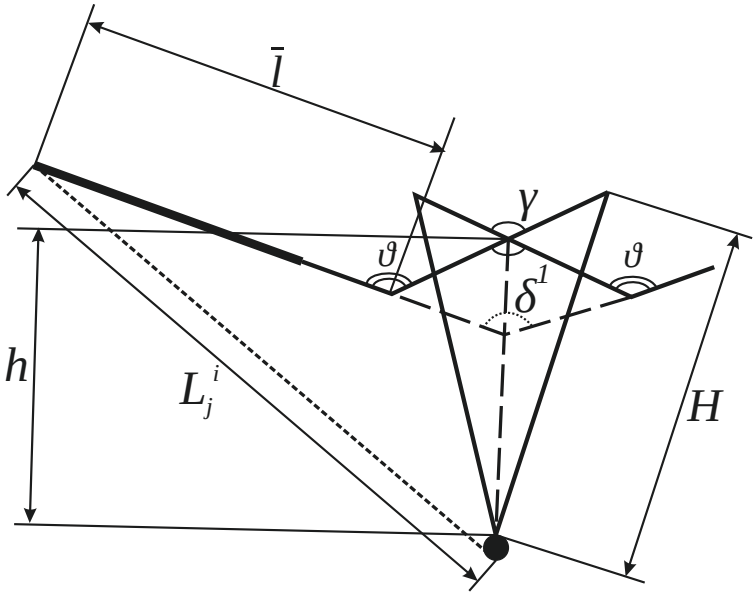

Fig. 3 – Model of V-folding rods

It is known that friction in pulley bearings decreases the cable tension. Taking this into account, the tension of adjacent sections of the cable can be given as follows:

$$T_{j+1}^{i} = \eta_j^i \cdot T_j^i \text{ for } j = 1,2; T_{j-2}^{i+1} = \eta_j^i \cdot T_j^i \text{ for } j = 3, i = 1,...,2, \tag{9}$$

where η_j^i is the tension decay factor for j-th pulley i-th section, and T_j^i is the tension force of the cable segment before j-th pulley i-th section.

The friction torque M occurs when a pulley rotates of around its bearing. According to the classical empirical Palmgrem equation, the magnitude of the friction torque can be expressed as:

$$M = f_1 F_\beta d_m, \tag{10}$$

where f_1 is a constant coefficient, F_β is the synthetic load, which for the ball bearing will be equal to the radial force F_r. Since all bearings in the structure are the same, pitch-circle diameter of the bearing d_m is also a constant. Then equation (10) can be written as follows:

$$M = fF_r, \tag{11}$$

where $f = f_1 d_m$ is a constant coefficient.

According to Newton's second law and the momentum theorem, the dynamics equation of the pulley can be written as:

$$T_j^i + T_{j+1}^i + F_r - m_p a_c = 0, \tag{12}$$

$$R \times T_j^i + R \times T_{j+1}^i + M - \frac{1}{2} m_p |R|^2 \frac{d\omega}{dt} = 0, \tag{13}$$

where a_c is an acceleration of the centroid of the pulley, m_p is a mass of the pulley, M is a friction moment on the pulley, ω is an angular velocity of the pulley and R is the radius of the pulley.

Given that the mass and diameter of the pulley are small, so its influence can be neglected. Compared with the driving force, equation (12) can be reduced to:

$$T_j^i + T_{j+1}^i + F_r = 0. \tag{14}$$

Since $|R|$ and $d\omega/dt$ also small, quadratic term $|R|$ can also be omitted, and then equation (23) can be rewritten as:

$$R \times T_j^i + R \times T_{j+1}^i + M = 0. \tag{15}$$

From equations 14 and 15, we can get:

$$F_r^2 = T_j^{i\,2} + T_{j+1}^{i\;2} + 2T_j^i T_{j+1}^i \cos\alpha_j^i, \tag{16}$$

$$\left(T_j^i - T_{j+1}^i\right)R - fF_r = 0, \tag{17}$$

where α_j^i is the angle between adjacent segments of the cable.

Then, using equations (16) and (17), the driving force equation can be expressed as:

$$\left(T_j^i - T_{j+1}^i\right)R - f\sqrt{T_j^{i\,2} + T_{j+1}^{i\;2} + 2T_j^i T_{j+1}^i \cos\alpha_j^i} = 0. \tag{18}$$

Using the results from Ref. [6], the tension decay factor can be determined as follows:

$$\eta_j^i = \frac{R - f \cdot \cos\left(\alpha_j^i / 2\right)}{R + f \cdot \cos\left(\alpha_j^i / 2\right)}. \tag{19}$$

Assuming that at each time moment the angles δ^i between the V-folding rods are known and taking into account the model shown in Fig. 3, the angles α_j^i can be found as follows:

$$\alpha_1^1 = \pi/2 - \gamma^1;$$

$$\alpha_j^i = \pi - 2\gamma^i,\ j = 2,\ i = 1,2;$$

$$\alpha_j^i = \pi - \gamma^i,\ j = 1,3,\ i = 1,2;$$

$$\gamma^i = arctg\left(\frac{\tilde{l}\,\sin\left(\left(\pi - \delta^i\right)/2\right) + h}{\tilde{l}\,\cos\left(\left(\pi - \delta^i\right)/2\right)}\right), \tag{20}$$

where $\tilde{l}$ is the length of the equivalent V-folding rod; h is the distance between the rotation axis of the pulley on the V-folding rods and the conditional point of V-folding of the rods.

Taking into account the model presented in fig. 3, the distance h can be found as follows:

$$h = H \cdot \sin^{-1}\left(\left(2\vartheta - \delta^i\right)/2\right), \tag{21}$$

where ϑ is the angle between the V-folding rod and the hinge element of the V-folding rods; H is the length of the hinge element of the V-folding rods.

$$T_j^i = EA\Delta L_j^i / L_j^i \,, T_j^{i+1} = \eta_j^i EA\Delta L_j^i / L_j^i \,, \tag{22}$$

E is Young's modulus of the cable, A is the area of the cable cross section, L_j^i is the neutral length of the cable segment, ΔL_j^i is the elongation of the cable span.

The elongations of the cable spans can be given as follows:

$$\Delta L_2^1 = \eta_2^1 \frac{L_2^1}{L_1^1} \Delta L_1^1, \tag{23}$$

$$\Delta L_3^1 = \eta_1^1 \eta_2^1 \frac{L_2^1 L_2^1}{L_1^1} \Delta L_1^1, ..., \Delta L_3^2 = \prod_{i=1}^{2} \prod_{j=1}^{3} \left(\eta_j^i\right) \frac{\prod_{i=1}^{2} \prod_{j=1}^{3} \left(L_j^i\right)}{L_1^1} \Delta L_1^1. \tag{24}$$

The total elongation of the cable can be obtained as the sum of the elongations of all cable spans of the system:

$$\Delta L_\Sigma = \left(1 + \left(\eta_1^1 L_2^1 + \eta_1^1 \eta_2^1 L_2^1 L_3^1 + ... + \prod_{i=1}^{2} \prod_{j=1}^{3} \left(\eta_j^i\right) \prod_{i=1}^{2} \prod_{j=1}^{3} \left(L_j^i\right)\right) \Big/ L_1^1\right) \Delta L_1^1. \tag{25}$$

Knowing the length of the cable wound on the winch ΔL_w the elongation of the first cable span can be found as follows:

$$\Delta L_1^1 = \left(1 + \left(\eta_1^1 L_2^1 + \eta_1^1 \eta_2^1 L_2^1 L_3^1 + ... + \prod_{i=1}^{2} \prod_{j=1}^{3} \left(\eta_j^i\right) \prod_{i=1}^{2} \prod_{j=1}^{3} \left(L_j^i\right)\right) \Big/ L_1^1\right)^{-1} \cdot \tag{26}$$
$$\cdot \left(\sum_{i=9}^{2} \sum_{j=1}^{3} L_j^i - L_0 + \Delta L_w^{i1}\right)$$

where L_0 is the neutral length of the cable at the initial moment of the deployment.

The neutral length of the cable spans L_1^i does not change during deployment. The neutral length of other segments can be determined as follows:

$$L_j^i = \sqrt{\left(l \cdot tg\vartheta\right)^2 + \left(H \cdot \sin^{-1}\left(\left(2\vartheta - \delta^i\right)/2\right)\right)^2} \,, \tag{27}$$

where l is the length of the V-folding rod.

After finding the elongation of the first span of the cable ΔL_1^1 using equation (14), the tension on this span can be found using expression (11). Equations (9) allow us to determine the tensions of other cable spans. After that, the equivalent forces acting in the corresponding nodes of the structure are determined as follows:

$$F_1^1 = \left[0; T_2^1 \cos\gamma^1; T_1^1 - T_2^1 \sin\gamma^1\right]^T, \tag{28}$$

$$F_1^2 = \left[0; -T_2^2 \cos\gamma^2 + T_1^2; -T_2^2 \sin\gamma^2\right]^T, \tag{29}$$

$$F_2^i = \left[0; \left(-T_2^i + T_3^i\right) \cdot \cos\gamma^i; \left(T_2^i - T_3^i\right) \cdot \sin\gamma^i\right]^T, \tag{30}$$

$$F_3^i = \left[0; -T_3^i \cos\gamma^i + T_1^{i+1}; -T_3^i \sin\gamma^i\right]^T. \tag{31}$$

Simulation results. The deployment of the considered structure was simulated using the models derived in Sections 4, 5 and the initial data presented in Table 1. The models were implemented using the open source software package HotInt [20].

The length of the cable wound on the winch varies as follows

$$\Delta L_w = 0.01t, \tag{32}$$

where t is the simulation time.

Figure 4 shows variations of the neutral lengths of the cables in the spans between the first and second pulleys. When the cables are being wound using the law (32), the they may sag (Fig. 5) and lose their tensions (Fig. 8) on some time interval. Figures 6, 7 demonstrate the variations of the cable tension decay factors during deployment. Figures 9, 10 show the dependences of the equivalent forces of the first and second pulleys of the second span over time, which lead to a change in the angles between the V-folding rods shown in fig. 11. As can be seen from the last figure, the considered cable winding law ensures the complete deployment of the structure in approximately 35 seconds.

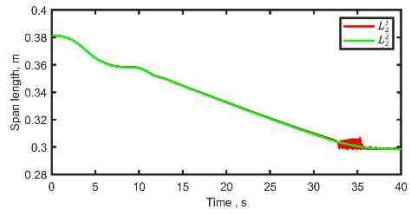

Fig. 4 – Variations of the neutral lengths of the cable spans between the pulleys

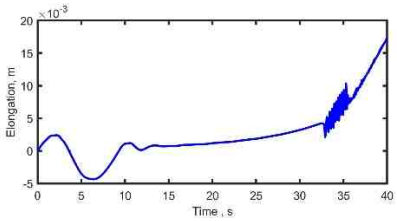

Fig. 5 – Variation of cable elongation

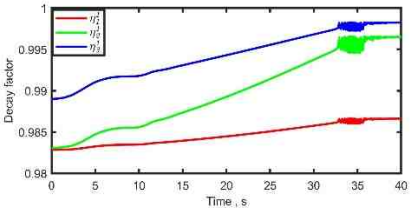

Fig. 6 – Variation of the tension decay factors for the first section of the structure

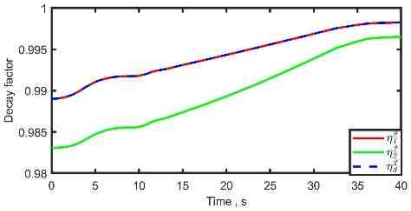

Fig. 7 – Variation of the tension decay factors for the second section of the structure

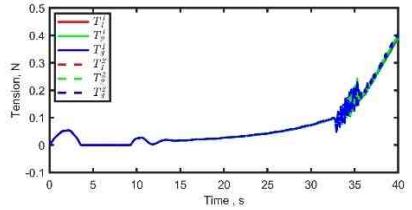

Fig. 8 – Variations of the cable tensions

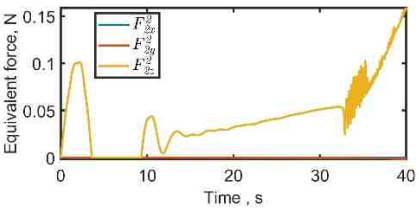

Fig. 9 – Variation of the equivalent force on the first pulley

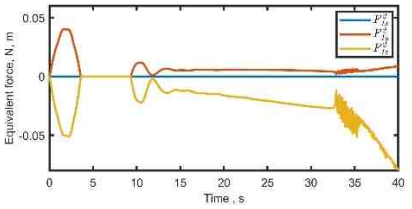

Fig. 10 – Variation of the equivalent force on the second pulley

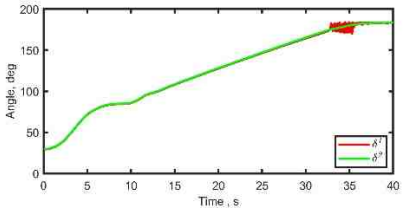

Fig. 11 – Variation of the angles between the V-folding rods

Conclusions. The article presents a model of the rod structure deployed by means of a cable-pulley system. A simplified method for modeling cable-pulley deployment systems has been developed, which allows calculating the cable tensions and nodal driving forces taking into account friction and other features of the system. The results of the calculations show that if the cable is wound at a constant speed, it can significantly lose tension or even sag at a certain time interval. Aa a result of this behavior the cable can lose contact the pulleys, which can lead to deployment failures. To eliminate the possible of sagging of the cables, they can be wound at a variable speed, using the obtained dependencies to determine the tension of the cable based on measurements of the angles between the folding rods. The development of such control algorithms may be the subject of further research.

1. *Duan B., Zhang Y., Du J.* Large Deployable Satellite Antennas: Design Theory. Methods and Applications Springer Nature. 2020. 271 pp. https://doi.org/10.1007/978-981-15-6033-0
2. *Khoroshylov S., Shamakhanov V., Vasyliev V.* Modeling of centrifugal deployment of three-section minisatellite boom. Technical mechanics. 2021. No. 4. Pp. 56–65. https://doi.org/10.15407/itm2021.04.056
3. *Peng Y, Zhao Z., Zhou M., He J., Yang J., Xiao Y.* Flexible Multibody Model and the Dynamics of the Deployment of Mesh Antennas. Journal of Guidance, Control, and Dynamics. 2017. V. 40, No.6. Pp. 1499–1510. https://doi.org/10.2514/1.G000361
4. *Liu L., Shan J., Tao C.* 2nd AIAA Spacecraft Structures Conference. https://doi.org/10.2514/6.2015-0947
5. *Jiang X., Bai Z.* Dynamics Modeling and Simulation for Deployment Characteristics of Mesh Reflector Antennas . Applied Sciences. 2020. V. 10(21). https://doi.org/10.3390/app10217884
6. *Liu L., Shan J., Zhang Y.* Dynamics Modeling and Analysis of Spacecraft with Large Deployable Hoop-Truss Antenna. Journal of spacecraft and rockets. 2016. V.53, No.3. https://doi.org/10.2514/1.A33464
7. *Peng H., Li F., Kan Z., Liu P.* Symplectic Instantaneous Optimal Control of Deployable Structures Driven by Sliding Cable Actuators. Journal of Guidance, Control, and Dynamics. 2020. V.43, No.6. Pp. 1114–1128. https://doi.org/10.2514/1.G004872
8. *Spiegelhauer M., Schlecht B.* Efficient modelling of flexible cable-pulley systems. Forsch Ingenieurwes. 2021. V.85. Pp. 67–75. https://doi.org/10.1007/s10010-020-00433-y
9. *Qi Z., Wang J., Wang G.* An efficient model for dynamic analysis and simulation of cable-pulley systems with time-varying cable length. Mechanism and Machine theory. 2017. V. 116. Pp. 383–403. https://doi.org/10.1016/j.mechmachtheory.2017.06.009
10. *Fu K., Zhao Z., Ren G., Xiao Y., Feng T., Yang J., Gasbarri P.* From multiscale modeling that design of synchronization mechanisms in mesh antennas. Acta Astronautica. 2019. V. 159. Pp. 156–165. https://doi.org/10.1016/j.actaastro.2019.03.056
11. *Zhang Y., Yang D., Sun Z et al.* Winding strategy of driving cable based he dynamic analysis of deployment for deployable antennas. J Mech Sci Technol. 2019. V.33. Pp. 5147–5156. https://doi.org/10.1007/s12206-019-0906-9

12. *Khoroshylov S., Shamakhanov V. et al.* Dynamics modeling and analysis of the deployable reflector antenna for SAR mini-satellites, 41st ESA Antenna Workshop, 25 – 28 September, Noordwijk, The Netherlands, 2023. https://www.researchgate.net/publication/374544077_DYNAMICS_MODELLING_AND_ANALYSIS_OF_THE_DEPLOYABLE_REFLECTOR_ANTENNA_FOR_SAR_MINI-SATELLITES
13. *Sushko O., Medzmariashvili E., Tserodze S. et al.* Design and Analysis of Light-Weight Deployable Mesh Reflector Antenna for Small Multibeam SAR Satellite, EUSAR 2021: Proceedings of the European Conference the Synthetic Aperture Radar, 29 March – 01 April 2021. Pp. 421–423.
14. *Alpatov A., Gusynin V., Belonozhko P. et al.* Shape control of large reflecting structures in space. 62nd International Astronautical Congress, 3–7 October Cape Town, South Africa, 2011. Pp. 5642–5648.
15. *Alpatov A., Gusynin V., Belonozhko P., Khoroshylov S., Fokov A.* Configuration modeling of cable-stayed space reflectors. Proceeding of the 64th International Astronautical Congress, Beijing, China, 2013. Pp. 5793–5799.
16. *Sushko O., Medzmariashvili E., Filipenko F. et al.* Modified design of the deployable mesh reflector antenna for mini satellites. CEAS Space J. 2021. Vol.13, No.4. Pp. 533–542. https://doi.org/10.1007/s12567-020-00346-0
17. *Khoroshylov S., Martyniuk S., Sushko O. et al.* Dynamics and attitude control of space-based synthetic aperture radar. Nonlinear Eng. 2023.V.12(1). https://doi.org/10.1515/nleng-2022-0277
18. *Shabana A.* Definition of ANCF Finite Elements. Journal of Computational and Nonlinear Dynamics. 2015. V.10. https://doi.org/10.1115/1.4030369
19. *Sautter K., Meßmer M., Teschemacher T., Bletzinger K.* Limitations of the St. Venant -Kirchhoff material model in large strain regimes. International Journal of Non-Linear Mechanics. 2022. V.147. https://doi.org/10.1016/j.ijnonlinmec.2022.104207
20. *Gerstmayr J., Dorninger A., Eder R. et al.* HOTINT: A Script Language Based Framework for the Simulation of Multibody Dynamics Systems. ASME IDETC/CIE. 2013. Vol.7B. https://doi.org/10.1115/DETC2013-12299

Received on November 13, 2023,
in final form on December 1, 2023